

## Journal Pre-proof

Surface modified Genistein phytosome for Breast Cancer Treatment: In-vitro Appraisal, Pharmacokinetics, and In-vivo Antitumor Efficacy

Ibrahim A. Komeil , Ossama Y. Abdallah , Wessam M. El-Refaie

PII: S0928-0987(22)00182-8  
DOI: <https://doi.org/10.1016/j.ejps.2022.106297>  
Reference: PHASCI 106297



To appear in: *European Journal of Pharmaceutical Sciences*

Received date: 1 June 2022  
Revised date: 7 September 2022  
Accepted date: 21 September 2022

Please cite this article as: Ibrahim A. Komeil , Ossama Y. Abdallah , Wessam M. El-Refaie , Surface modified Genistein phytosome for Breast Cancer Treatment: In-vitro Appraisal, Pharmacokinetics, and In-vivo Antitumor Efficacy, *European Journal of Pharmaceutical Sciences* (2022), doi: <https://doi.org/10.1016/j.ejps.2022.106297>

This is a PDF file of an article that has undergone enhancements after acceptance, such as the addition of a cover page and metadata, and formatting for readability, but it is not yet the definitive version of record. This version will undergo additional copyediting, typesetting and review before it is published in its final form, but we are providing this version to give early visibility of the article. Please note that, during the production process, errors may be discovered which could affect the content, and all legal disclaimers that apply to the journal pertain.

© 2022 Published by Elsevier B.V.  
This is an open access article under the CC BY-NC-ND license  
(<http://creativecommons.org/licenses/by-nc-nd/4.0/>)

**Surface modified Genistein phytosome for Breast Cancer Treatment: *In-vitro* Appraisal, Pharmacokinetics, and *In-vivo* Antitumor Efficacy**

By

Ibrahim A. Komeil<sup>1\*</sup>, Ossama Y. Abdallah<sup>2</sup>, Wessam M. El-Refaie<sup>1</sup>

<sup>1</sup> Department of Pharmaceutics, Faculty of Pharmacy, Pharos University in Alexandria, Alexandria, Egypt.

<sup>2</sup> Department of Pharmaceutics, Faculty of Pharmacy, Alexandria University, Alexandria, Egypt.

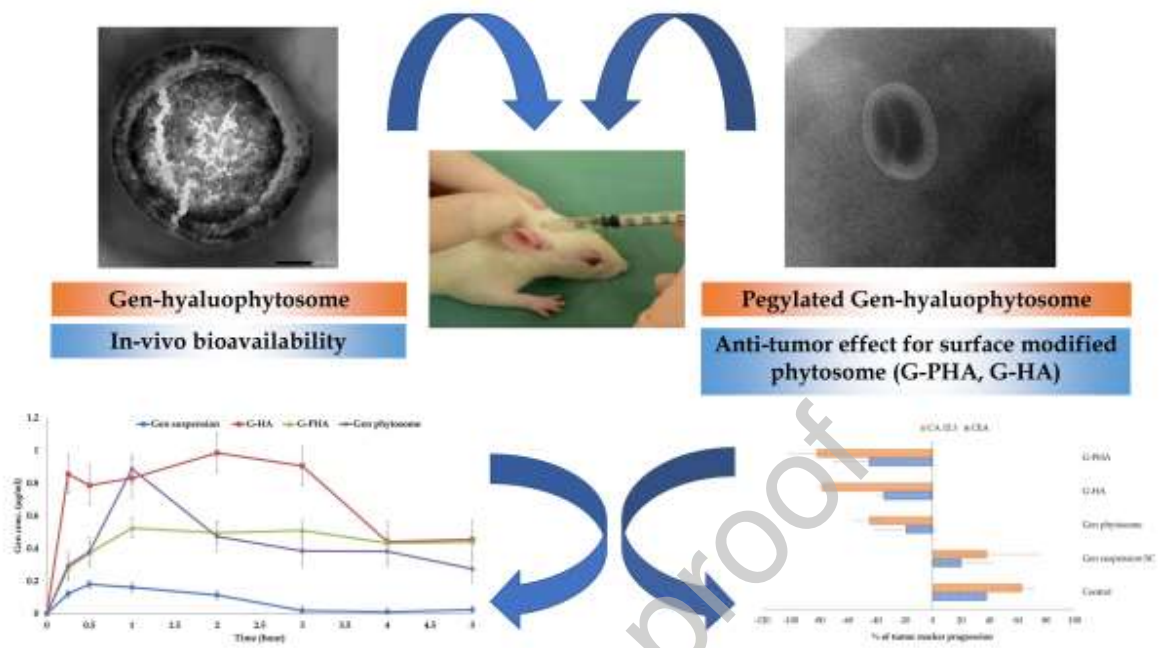
\*Corresponding author, Department of Pharmaceutics, Faculty of Pharmacy, Pharos University in Alexandria, Alexandria, Egypt.

**Tel: 002 01005238469**

**E-mail: ibrahimkomeil393@gmail.com**

**The authors report no financial or personal conflict of interest.**

Graphical abstract



## Abstract

Based on phytosomes advantages over liposomes, hyaluronic acid (HA) with/out pegylated phospholipid was used to develop surface-modified genistein (Gen) phytosome as Gen pegylated hyaluophytosomes (G-PHA) and Gen hyaluophytosomes (G-HA) as novel delivery systems for breast cancer treatment. In this study, *in-vitro* characterization of G-HA and G-PHA shows PS  $144.2 \pm 1.266$  nm and  $220.3 \pm 2.51$  nm, ZP  $-30.9 \pm 0.75$  and  $-32.06 \pm 0.305$  respectively. Morphological elucidation shows HA covers the surface of G-HA and the presence of a transparent layer of PEG surrounding G-PHA. *In-vitro* release shows a significant slow Gen release from G-HA, and G-PHA compared to Gen solution and Gen phytosomes. *In-vivo* bioavailability data shows improvement in bioavailability for G-HA and G-PHA compared to Gen suspension ( $AUC_{0-t}: 3.563 \pm 0.067$ ,  $2.092 \pm 0.058$ ,  $0.374 \pm 0.085$   $\mu\text{g/ml}\cdot\text{h}$  respectively). Therapeutic evaluation of the prepared targeted formulations was carried out by subcutaneous injection in an EAC-induced breast cancer model in mice. G-HA and G-PHA show a promising chemotherapeutic effect in terms of lowering the tumor size and tumor biomarkers (CEA:  $-34.6$ ,  $-44.7$  & CA15.3:  $-77.8$ ,  $-81.6$  respectively). This reduction in their values compared to Gen phytosomes, Gen suspension, and the control group is attributed to high Gen accumulation at the target organ owing to targeting properties of HA that are used in phytosomal surface modification in G-HA. Additionally, the presence of MPEG<sub>2000</sub>-DSPE in G-PHA tends to improve interstitium lymphatic drainage following SC administration, resulting in maximizing the therapeutic benefits of breast cancer despite the difference in pharmacokinetics behavior compared to G-HA. These formulations can be further studied for metastatic breast cancer.

**Keywords:** Genistein, hyaluronic acid, Gen hyaluophytosome, pegylated hyaluophytosome lymphatic delivery, breast cancer

## 1. Introduction

Breast cancer is the most common metastatic cancer among women and is considered one of the leading causes of morbidity and mortality worldwide. It is categorized into three major subtypes based on the presence or absence of molecular markers estrogen or progesterone receptors and human epidermal growth factor 2 (ERBB2; formerly HER2) including hormone receptor-positive/ERBB2 negative (70% of patients), ERBB2 positive (15%-20%) and triple-negative (tumors lacking all 3 standard molecular markers; 15%<sup>(1)</sup>). Lymphatic vessels are characterized by high permeability compared to vascular vessels. Therefore, the lymphatic system serves as the primary route for tumor cell metastasis. Where tumor cells migrate from the primary tumor to the sentinel lymph node. Eventually, it exits via the efferent lymphatic vessels and utilizes the venous system or the nascent blood vessels that serve lymph nodes to merge with the systemic circulation<sup>(2)</sup>.

Genistein (Gen) is a polyphenolic isoflavone, which has a close structural similarity to estrogens. Gen has weak estrogenic activity and is labeled as a phytoestrogen. Because of its structural similarity to 17 $\beta$ -estradiol (estrogen), Gen has been shown to compete with 17 $\beta$ -estradiol in ER (estrogen receptor)<sup>(3)</sup>. Gen blocks the binding site of more potent estrogens at the same time it affects estrogen metabolism, thereby exerting a potentially favorable role in the prevention of breast

cancer. Additionally, Gen is a well-known inhibitor of the protein-tyrosine kinase (PTK) which may suppress the growth of cancer cells by inhibiting PTK-mediated signaling mechanisms<sup>(4)</sup>. Sakla et al.<sup>(5)</sup> reported that Gen inhibits the proto-oncogene HER-2 protein tyrosine phosphorylation in breast cancer cells as well as delaying tumor onset in transgenic mice that overexpress the HER-2 gene. However, Gen possesses poor aqueous solubility and extensive hepatic metabolism<sup>(6)</sup> which limits its clinical application. Recently, Bhat et al<sup>(7)</sup> showed other cytotoxic effects of Gen against breast cancer. Therefore, the use of a targeted drug delivery system is a promising approach to delivering active Gen aglycone to breast cancer cells.

Tyagi et al<sup>(8)</sup> proposed different delivery systems that were developed to solve the biopharmaceutical obstacles facing Gen development from bench to clinic including polymeric nanoparticle<sup>(9-13)</sup>, nanocapsule<sup>(14)</sup>, nanoemulsion<sup>(15,16)</sup>, nano lipid carrier<sup>(17)</sup> and metallic nanoparticle<sup>(18)</sup>. *In-vitro* cytotoxicity rather than *in-vivo* cytotoxicity evaluation was applied only for those delivery systems. They were assessed in different cancer models including cervical, liver, colon, prostate, and human lung carcinoma.

Phospholipid-based delivery systems such as liposomal nanocarriers attracted much interest in lymphatic delivery after subcutaneous (SC) injection. Vesicle size, liposome composition, surface charge<sup>(19-21)</sup>, and steric stabilization of liposome may enhance lymphatic drainage<sup>(22)</sup>. Tiantian et al.<sup>(23)</sup> reported using soy phosphatidylcholine (SPC) in the preparation of low molecular weight hyaluronic acid-modified docetaxel-loaded liposomes to enhance lymphatic drainage and lymph node uptake of liposomes following SC administration.

Unlike liposome, phytosome is a chemical interaction between phospholipid molecule and polyphenolic compound either by hydrogen bond formation or by van der Waal attraction force. Therefore, drug leakage in phytosomal formulations does not take place<sup>(24)</sup>. Additionally, the physicochemical stability of phytosome depends on the physicochemical properties of the drug-lipid complex, such as phase transition temperature, solubility, melting point, and lipid composition which results in better physical stability over conventional liposomes<sup>(25)</sup>. However, not enough studies were performed on using surface-modified phytosomes as a targeting delivery system.

Hyaluronic acid (HA) is a negatively charged hydrophilic biocompatible polymer of linear glycosaminoglycan and it's the major component of the extracellular matrix and is distributed in various body parts<sup>(26)</sup>. It is reported to be used in breast cancer cell targeting as it is one of the most important ligands for CD44 receptors found at the surface of a breast cancer cell<sup>(27)</sup>. Where CD44 receptor is activated in the presence of HA resulting in a series of cellular events leading to increased cell proliferation and migration. Interestingly, It is proposed that HA follows lymphatic drainage from the interstitium like natural compounds<sup>(23)</sup>. PEGylation technique is used in different liposomal research work for breast cancer targeting to achieve prolonged drug circulation in plasma and controlled release *in vivo* after intravenous administration<sup>(28)</sup>. Additionally, PEGylated

liposomes would hamper the phagocytosis by macrophages and influence their uptake by the lymph node owing to the presence of a PEG hydrophilic layer that possesses steric stabilization<sup>(19)</sup>

Our study aims to develop a novel surface modified Gen-phytosomes for *in-vivo* breast cancer treatment using biocompatible excipients. As a chosen ligand, HA was used to prepare (Gen hyaluophytosomes, G-HA) to direct Gen phytosome to the highly CD44 expressed breast tumor however, PEGylated phospholipid (MPEG<sub>2000</sub>-DSPE) was also used to prepare (Gen pegylated hyaluophytosomes, G-PHA) to enhance the lymphatic drainage of Gen HA. G-HA and G-PHA were characterized *in-vitro* for their quality attributes. *In-vivo* characterization includes the effect of the surface-modified formulations on Gen pharmacokinetics. The therapeutic effectiveness was also evaluated following SC administration.

## 2. Materials and methods

### 2.1. Materials

Genistein (Gen) powder was purchased from Shanghai-Soyoung Biotech. Inc (Shanghai, China). Lipoid® S100 (~98% pure soy phosphatidylcholine SPC) and 2-dioleoyloxy-3-Trimethylammoniumpropanchloride (DOTAP) and Lipoid PE 18:0/18:0-PEG 2000 (N-(Carbonyl-methoxy polyethylene glycol-2000)-1, 2 distearoyl-sn-glycero-3 phosphoethanolamine, sodium salt) MPEG<sub>2000</sub>-DSPE were gift samples from Lipoid Co., Ludwigshafen (Germany). Low molecular weight Hyaluronic acid [Mwt = 0.8-1.17 x 10<sup>4</sup> Da] was a sample gift from Shiseido (Japan). Propylparaben base was a sample gift from Medizen Pharmaceutical Industries, Egypt. Methanol and Acetonitrile HPLC were purchased from J.T.Baker (USA). 0.85% Phosphoric acid, acetic anhydride, glacial acetic acid, ammonium acetate, and Diethyl ether were purchased from Loba Chemie (India).

### 2.2. Animals

Female albino mice (25 - 30 gm) were obtained from the animal house (Pharos University, Alexandria) to be used in the experiments. All experiments were held under the National Institute of Health guide for the care and use of laboratory animals and ethically approved by the unit of research ethics approval committee (Pharos University, Alexandria, #01201910133011). The mice were housed in a temperature and humidity-controlled room (23°C, 55% air humidity) with free access to water and standard chow. Mice were fed with non-soy food for at least one week before the experiments<sup>(29)</sup> and were fasted overnight before the date of any experiment with free access to water.

### 2.3. Preparation of surface-modified Gen-phytosomes

Gen-SPC complex was previously prepared and physically characterized to elucidate the complex formation between Gen and SPC namely, Lipoid® S 100<sup>(30)</sup>. Using the solvent evaporation method<sup>(31,32)</sup> Gen (20 mg) and SPC (molar ratio 1:4.5) were dissolved in 25 ml of methanol at room temperature. Then, the mixture was subjected to evaporation in a thermostatically controlled water bath (37±1 °C) for 12-14 hours. *In-vitro* characterization of the Gen-SPC complex was carried out

using differential scanning calorimetry (DSC) and Fourier transform infrared (FT-IR). Gen powder, pure SPC, Gen-SPC, and physical mixture were used in those measurements.

### *2.3.1. Preparation of Gen-loaded hyaluophytosomes (G-HA)*

Based on the former Gen-SPC complex preparation method, DOTAP was added in different weight percentages relative to SPC (0.075%, 1%, and 2%). The mixture was refluxed for 2 hours in 25 ml methanol at room temperature. To obtain G-HA; 100 ml HA solution (pH 7.4 PBS) in different concentrations (0.05, 0.1, 0.2 mg%) was kept at 25 °C with 20 rpm magnetic stirring. A positively charged Gen-SPC-DOTAP complex was slowly added to the above HA solution under vigorous stirring. After completion of the addition step, stirring was continued for 10 minutes<sup>(23)</sup>.

### *2.3.2. Preparation of Gen-loaded pegylated hyaluophytosomes (G-PHA)*

The abovementioned method of preparation was used and MPEG<sub>2000</sub>-DSPE has been added to Gen-SPC-DOTAP (1:4.5:0.045) mixture with a mass ratio (1:1) to DOTAP<sup>(33)</sup>. To obtain G-PHA phytosomes, the prepared complex was added slowly with 0.1% of aqueous HA (pH 7.4 PBS) under vigorous stirring. The stirring was continued at 20 rpm and 25 °C for 10 minutes. The prepared G-HA and G-PHA formulations were extruded for 5 successive cycles through a polycarbonate membrane (pore size of 200 nm, 25 mm diam.) at room temperature with the aid of a liposome extruder (Model ER-1, Eastern scientific LLC, USA) and were filled into tightly capped tubes and stored at 4°C.

## **2.4. In-vitro characterization of surface-modified Gen phytosomes**

### *2.4.1. Analysis of Gen content in the prepared formulations*

A sample equivalent to 20 mg Gen from the prepared phytosomes (Gen phytosome, G-HA, and G-PHA) was dissolved in 100 ml methanol. After proper dilution, Gen concentration was measured by validated HPLC measurement<sup>(34)</sup>. HPLC (Agilent 1200, USA) supplied with a UV-diode array detector was used with the Hyperclone™ BDS C18 column (5µm, 130Å, 250 x 4.6 mm). 20µl of samples were eluted with a solvent mixture of 50 mM of ammonium acetate buffer and acetonitrile using gradient elution with a 1.5 ml/min flow rate and 37 minutes runtime. The UV detection wavelength was set at 250 nm.

### *2.4.2. Particle size, Zeta potential, and polydispersity index*

The mean particle size (PS), polydispersity index (PDI), and zeta potential (ZP) for the prepared Gen phytosome, G-HA, and G-PHA formulations were measured after 250 fold dilution with filtered diluted PBS pH 7.4 by using the dynamic light scattering technique (DLS) using Malvern zetasizer (Malvern instruments, UK). Measurements were performed in triplicates. Data are presented as mean value ± SD.

#### 2.4.3. Morphological elucidation by transmission electron microscope (TEM)

The morphological examination was carried out on Gen phytosome, G-HA, and G-PHA. A single drop from each sample was added to a copper grid then excess fluid was removed by a piece of filter paper. The film on the grid was subsequently stained using uranyl acetate and allowed to dry at room temperature before the TEM examination<sup>(35)</sup>.

#### 2.4.4. In-vitro drug release study

The dialysis method was used to assess and compare the release of Gen from its solution, an aqueous dispersion of Gen-phytosomes, G-HA, and G-PHA in comparison with Gen suspension. Dialysis bags (Visking<sup>®</sup>, diameter 21 mm, MWCO 12000-14000, Serva, USA) were filled with 1 ml sample containing 0.3 mg/ml Gen and placed in 23 ml of phosphate buffer pH 6.8 and 0.1% (w/v) tween 80 as the release medium under sink conditions as described by shehata et al<sup>(36)</sup>. The experiment was performed in a thermostatically controlled shaking water bath equipped at 37±0.5°C and 100 rpm. At different time intervals (0.5, 1, 2, 3, 4, 5, and 24 hours), 1 ml sample was withdrawn and replaced with the same volume of prewarmed fresh release medium. Samples were assayed by HPLC. All experiments were performed in triplicate and the results are presented as mean value ± SD.

#### 2.5. In-vivo bioavailability study

To figure out the effect of Gen phytosomes, G-HA, and G-PHA on Gen systemic bioavailability after SC administration; pharmacokinetic parameters were calculated for parent unconjugated Gen (free aglycone) applying a non-compartmental model using PK Solver Add-ins tool in Microsoft<sup>®</sup> Excel 2016. Pharmacokinetic parameters such as  $C_{max}$  and  $AUC_{0-t}$  were calculated applying a trapezoidal rule.

0.4 ml of Gen phytosome, G-HA, and G-PHA formulations compared to Gen suspension were injected with SC providing 50 mg Gen /Kg to detect the parent aglycone in different biological matrices. Healthy female mice were divided into 4 groups for Gen suspension, Gen-phytosome, G-HA, and G-PHA (5 mice/group) and anesthetized with Diethyl Ether.

Blood samples (200–300 µL) were collected from a super facial temporal vein after 0.25, 0.5, 1.0, 2.0, 3.0, 4.0, and 5.0 hours in polyethylene tubes supplied with K<sub>2</sub>EDTA. Blood samples were subjected to centrifugation at 4000 rpm at room temperature to separate plasma. Plasma samples were stored in a deep freezer (-20°C) until analysis. Samples were assayed using HPLC analysis with propylparaben (PP) as an internal standard (IS)<sup>(34,37)</sup>. All experiments were performed in triplicate and the results are presented as mean value ± SD.

#### 2.6. Antitumor activity of surface-modified Gen- phytosomes

Breast cancer was induced by SC injection of 0.2 ml of diluted Ehrlich Ascites Carcinoma (EAC) fluid containing a fixed number of viable cells. The fluid was injected into the left side of the mammary fat pad of female albino mice. Twenty-five mice were divided into 5 groups (5 mice/group).

The tumor growth was measured by using Vernier calipers and tumor volume was calculated using the following equation<sup>(38)</sup>:

$$V = (L \times W^2) \times 0.5$$

Where V = tumor volume, L = length and W = width.

After 7 days of EAC inoculation, tumor size was examined using calipers. Gen suspension, Gen phytosome and targeted Gen-phytosomes (G-HA and G-PHA) equivalent to (15mg Gen/kg) were subcutaneously injected into the flank for 10 days. Tumor growth inhibition was measured by using Vernier calipers at 7 and 17 days from EAC inoculation and tumor volume was calculated using the same equation illustrated before. The % change in tumor volume was calculated for all study groups. Animals were anesthetized with 20% Diethyl ether and blood samples were withdrawn into non-heparinized tubes for tumor marker analysis at zero, 7, and 17 days of EAC inoculation<sup>(39)</sup>. Tumor markers applied for breast cancer assessment were carcinoembryonic antigen (CEA) and cancer antigen (CA 15.3). At the end of the treatment, mice were sacrificed, and blood samples were collected by direct heart puncture. The infected mammary gland was isolated to be used in further experiments.

### 2.7. Gen disposition in isolated mammary gland

After animal sacrifice, mammary gland homogenate was used to determine Gen disposition in the mammary gland after the treatment period. Where it was weighed, and PBS (pH=7.4) was added in a ratio (1:1) before the homogenization step. 400  $\mu$ l of methanol and 100  $\mu$ l PP as internal standard were vortexed with the same amount of mammary gland homogenate. Samples were subjected to centrifugation at 15000 rpm for 5 minutes. The supernatant was carefully withdrawn and filtered through a 0.45  $\mu$ m syringe filter before being analyzed by HPLC. Samples were analyzed in triplicates and data were represented as mean value  $\pm$ SD.

### 2.8. Statistical data analysis

Statistical data analysis was carried out using (Graph prism, version 5, USA). Results were expressed using mean and standard deviation. Statistically significant differences were determined using a two-tailed unpaired student's t-test. For pairwise comparison, one-way ANOVA was followed by Tukey's post hoc analysis.  $P < 0.05$  was described as the level of significance.

## 3. Results & Discussion

CD44 receptor is overexpressed at the surface of breast cancer cells, and it involves different cell proliferation events. HA is a CD44 agonist, thus the modification strategy of Gen-phytosomes depended on developing Gen-hyaluophytosome formulation for breast cancer targeting. PEGylated hyaluophytosomes were also prepared using MPEG<sub>2000</sub>-DSPE to improve the lymphatic drainage for the targeted formulation. SC route of administration is considered also to be a primary route for lymphatic delivery with several advantages. These advantages include drug accumulation at the site of administration for a longer period, low clearance, sustained release, and increased absorption.

After SC administration, lipid nanoparticles (LNPs) are not directly transported to systemic circulation because capillaries control the permeability of water and small molecules. However, LNPs tend to be absorbed by lymphatic capillaries which surround the sub-cutaneous site of injection rather than systemic capillaries depending on their size, surface charge, and degree of hydrophilicity<sup>(40)</sup>.

### 3.1. Preparation and optimization of surface-modified Gen phytosomes

#### 3.1.1. Gen phytosomes

Different molar ratios between Gen and SPC were previously examined<sup>(30)</sup>, it is found that the molar ratio (1:4.5) between Gen and SPC results in the formation of clear yellow stable gel form preparation. The complex is further confirmed by utilizing FT-IR and DSC, figure (1).

As shown in figure (1A), a characteristic broad stretching band for Gen-SPC complex is observed at 3600-3100  $\text{cm}^{-1}$  referring to contributions of O-H stretching vibration arising from hydrogen bond with different O-H groups of Gen (i.e., sharp peak at 3400  $\text{cm}^{-1}$  for pure Gen<sup>(41)</sup>). Additionally, a characteristic sharp peak at 1299-1250 of P=O<sup>(42)</sup> in pure SPC is not observed in the complex. In figure (1B), an endothermal peak for the Gen-SPC complex is observed at 129.8 °C while the endothermal peak for Gen and SPC is appeared at 303.66 °C<sup>(43)</sup> and 162 °C, respectively. These observations indicate a formation of the complex between Gen and SPC by hydrogen bond formation between phenolic (-OH) groups and P=O of SPC. However, no change in IR spectra and DSC peaks for Gen and SPC are notified in a physical mixture between them.

#### 3.1.2. Gen-hyaluophytosome (G-HA)

The pKa of HA was approximately 3.0, thus ionization of HA is complete in the pH 7.4 PBS<sup>(23)</sup>. HA acquires a negative charge which hinders it to be electrostatically attached to the surface of the formed vesicles. It is observed that Gen-phytosomes acquire a negative net charge (i.e. -35mV $\pm$ 0.80) on their surface due to the presence of phosphate group in its chemical structure. Cationic liposomes are likely to be prepared by DOTAP<sup>(44)</sup>. DOTAP can convert the surface net charge to a positive charge owing to the presence of a quaternary ammonium group in its chemical structure. *In-vivo* toxicity of cationic liposomes induced by DOTAP was discussed previously by Knudsen et al. <sup>(44)</sup> supporting the use of DOTAP in the lowest applicable concentration use (0.75%, 1%, and 2% of SPC concentration).

The net surface charge of 0.75%, 1% and 2% DOTAP-SPC vesicles are measured to be (-35.9 mV $\pm$ 0.96, +22.6 mV $\pm$ 0.67 and +65.1 mV $\pm$ 0.82), respectively. Based on this; 1% DOTAP was used in the preparation of G-HA formulations complex to be hydrated with hyaluronic acid (HA) to form hyaluophytosomes.

Different concentrations of LMWHA in the hydrating medium (0.05%, 0.1%, and 0.2%) were examined to determine the appropriate amount of HA to be used in G-HA preparation. Where using low concentrations in the hydrating medium is reported to surround the vesicle surface<sup>(45)</sup>.

The net negative charge on the surface of phytosomes increases with HA concentration increase to be (-30.2 mV  $\pm$ 0.49, -35.6mV  $\pm$ 0.50, and -54.7 mV  $\pm$ 0.71) for 0.05%, 0.1%, and 0.2% LMWHA solutions respectively. This might be attributed to HA coating on the surface of phytosomes thus imparting a negative charge. 0.2% HA shows a significant ( $P < 0.05$ ) high negative charge than other concentrations indicating the presence of an excess amount of HA in the medium rather than the vesicle surface. Hence, using 0.1% HA was selected for efficient coating on the vesicle surface rather than dispersion medium.

### 3.1.3. Gen-pegylated hyaluophytosome (G-PHA)

To improve the effectiveness of Gen in cancer treatment owing to the presence of HA and polyethylene glycol (PEG), a novel formulation of Gen pegylated hyaluophytosomes was prepared. The preparation of pegylated liposomes was previously described by Yang et al.<sup>(46)</sup> to improve the passive targeting for pegylated paclitaxel-loaded liposomes via enhanced permeability and retention mechanism *in-vivo*<sup>(47-50)</sup>. It was reported by Zhuang et al.<sup>(33)</sup> that using 1mol% of MPEG<sub>2000</sub>-DSPE relative to DOTAP in cationic liposomes accelerated the drainage of DOTAP liposomes into draining lymph nodes and prolonged their lymph node retention following SC administration. Additionally, applying 5 mol% of MDPEG<sub>2000</sub>-DSPE into DOTAP liposomes enhanced their lymph node retention and uptake to a lesser extent.

PEG also prolonged the blood circulation of DOTAP liposomes and increased their splenic accumulation. Thus, 2.5 mol% of MPEG<sub>2000</sub>-DSPE was selected for the preparation of the Gen-SPC-DOTAP complex relative to DOTAP mol %. Then, Gen-SPC-DOTAP-MPEG<sub>2000</sub>-DSPE was dispersed after solvent evaporation in 0.1% HA to prepare pegylated Gen-hyaluophytosomes.

### 3.2. Characterization of surface-modified Gen phytosomes

Physicochemical characterization of targeted Gen phytosomes encompassed the assessment of Gen content, PS, ZP, and PDI as depicted in Table (1).

PS for G-HA showed a significantly lower ( $P < 0.05$ ) value (144.2 nm  $\pm$  1.266) compared to G-PHA (220.3 nm  $\pm$  2.516). This may be attributed to the presence of a layer of a PEG surrounding the phytosomal vesicle leading to an increase in its particle size compared to G-HA as presented in Table (1). The presence of HA in G-HA and G-PHA provided a negative charge for the whole dispersion system with no significant difference between them ( $P > 0.05$ ).

### 3.3. Transmission electron microscope

As shown in figure (2), TEM of Gen-phytosomes (2A), reveals a well-formed discrete vesicle with a well-identified phospholipid bilayer in different magnification powers.

G-HA shows a black disposition with a bright background on the surface of the spherical vesicles in figure (2B). Black disposition can be related to the presence of HA on the surface which turns in black because of staining with uranyl acetate. This finding is by Li et al. <sup>(51)</sup> who showed also using the uranyl acetate stain for HA. The cracks observed on the vesicle's surface shown in figure (2B) might be due to the drying step during the sample preparation processor or may be referred to as incomplete surface coverage with HA. Figure (2C) shows a TEM microscopic photograph for G-PHA, where a black spherical vesicle is appeared owing to the presence of HA as shown in figure (2C) with a white layer surrounding it. This might be attributed to the presence of PEG chain protrusion through the HA layer surrounding the phospholipid bilayer. These PEG chains may appear to form a hydrophilic sheath cover HA coating layer. It is observed the thickness of the bilayer for G-PHA reached 30.1 nm because of the presence of HA and PEG layer surrounding phytosome vesicles. PS measurements on TEM images are recorded microscopically using TEM and found to be 100 nm, 200 nm, and 100 nm for Gen phytosome, G-HA, and G-PHA, respectively. These findings differ from PS measurements by (Malvern<sup>®</sup>, USA) due to differences in measurement techniques.

#### 3.4. *In-vitro* drug release

Release data of Gen suspension was excluded from the results as the measurements were below the limit of quantification of Gen. As shown in figure (3), the initial release (0.5 – 4 hours) for Gen solution is significantly higher ( $P < 0.05$ ) than other Gen formulations. The release pattern for G-HA and G-PHA is significantly lower ( $P < 0.05$ ) than the Gen solution and Gen phytosome. This might be attributed to the presence of HA (0.1%) in the Gen hyaluophytosome dispersions. HA hinders the release of solubilized complexed Gen through the dialysis membrane. Additionally, there is a non-significant difference ( $P > 0.05$ ) between G-HA and G-PHA. G-HA showed slightly better release through the dialysis membrane than G-PHA. This may be attributed to the relatively larger particle size of pegylated phytosomes compared to G-HA phytosomes.

#### 3.5. *In-vivo* bioavailability study

The assay linearity of Gen calculated by measuring the peak area ratio of analyte to PP between the concentration range (0.11 to 24.96  $\mu\text{g/ml}$ ) showed high linearity with a mean  $r^2 \geq 0.992$ . The weighted slope and intercept were found to be  $y = 0.2245x + 0.123$ . The validation data showed the assay to be sensitive, accurate and precise with the intraday RSD% less than 9.88%. Whereas the intraday RSD% less than 3.55%. Figure (4) and table (2) show the bioavailability of Gen aglycone in blood and other pharmacokinetic data after SC injection of Gen suspension, Gen-phytosome, G-HA, and G-PHA.

Gen formulations (Gen phytosome, G-HA, G-PHA) show a statistically significant increase ( $P < 0.05$ ) in ( $\text{AUC}_{0-t}$ ) value over Gen suspension indicating an enhancement of *in-vivo* bioavailability for Gen formulations over Gen suspension. This may be attributed to Gen retention at the site of injection resulting in low plasma exposure where the net surface charge is neutral allowing the

formulations to be trapped at the site of injection rather than systemically absorbed as illustrated previously by Patel et al<sup>(52)</sup>.

Under influence of small particle size, negative surface charge, and hydrophilicity; Gen phytosomes tend to be absorbed systemically via interstitium lymphatic drainage as shown previously by Hawley et al<sup>(53)</sup>. However, G-HA shows a significant ( $P < 0.05$ ) higher  $AUC_{0-t}$  value compared to Gen-phytosome. This reflects a significant contribution of free HA in G-HA in improving Gen plasma exposure. These results align with those explained by Tiantian et al. <sup>(23)</sup> after SC administration of docetaxel liposome coated with HA. They postulated that increasing the molecular weight of free HA, will result in lymphatic drainage obstruction leading to increase Gen exposure in plasma.

Interestingly, G-PHA possesses significantly ( $P < 0.05$ ) lower values in  $AUC_{0-t}$ , compared to G-HA, indicating low Gen plasma exposure although small particle size, negative surface charge, and presence of HA in its formulation. This result may be referred to by many assumptions; slow drainage from the injection site compared to G-HA because of the high particle size of G-PHA injected particles (220.3 nm) compared to G-HA (144.2 nm). Additionally, the particle size of SC administered particles will significantly affect lymphatic uptake for injected particles as illustrated previously by Hawley et al.<sup>(53)</sup>. On the other hand, surface modification with PEG (G-PHA) leads to an increase in hydrophilicity of phytosomal vesicles. This results in the migration of vesicles through aqueous channels of the interstitium thus increasing its lymphatic uptake<sup>(20)</sup>. Being coated with a hydrophilic layer (PEG), hydrophilic G-PHA possesses a low phagocytic response by phagocytes in lymphatic circulation leading to prolongation in lymphatic circulation rather than captured by opsonin<sup>(54)</sup>. It is concluded from the discussion that G-PHA shows a low systemic circulation to be more prolonged in lymphatic circulation after SC administration. This will be further confirmed from the obtained *in-vivo* Gen deposition in mammary glands and its efficacy from G-HA and G-PHA.

### **3.6. *In-vivo* anti-tumor activity**

Anti-tumor activity for Gen against breast cancer was assessed after S.C administration of Gen suspension, Gen phytosome, G-HA, and G-PHA. Ehrlich ascites carcinoma (EAC) cell line was used previously in different research articles for estrogenic<sup>(55)</sup> breast cancer induction in balb/C female rats <sup>(27,56)</sup>. Being an estrogenic substrate, Gen suspension, Gen phytosome, and surface-modified Gen phytosomal formulations were assessed in the treatment of estrogenic breast cancer.

#### *3.6.1. Gen disposition in malignant mammary gland*

The therapeutic effect of Gen formulations will depend on Gen aglycone accumulation in the mammary glands. Results of Gen disposition in mammary glands from the different formulations indicated the significant ( $P < 0.05$ ) higher accumulation of Gen from G-HA and G-PHA compared

to Gen suspension and Gen phytosomes, figure (5, bars). In addition, a non-significant difference ( $P > 0.05$ ) was observed between G-PHA and G-HA groups in Gen accumulation in breast tissue despite the difference in their bioavailability performance.

### 3.6.2. Percentage of change in tumor size

Figure (5, line) shows the percentage of change in tumor size compared to the control group. A significant increase in tumor size in Gen suspension was observed compared to other Gen formulations. Additionally, there is a significant increase in tumor size for Gen phytosome group compared to surface-modified Gen phytosomal formulations. It can be concluded that the change in tumor size is correlated with the amount of Gen accumulated in the mammary gland which proves the effectiveness of surface-modified Gen phytosomal formulations in Gen delivery to the tumorous organ over un-modified Gen phytosome.

### 3.6.3. Tumor biomarkers (CA and CA 15.3)

As shown in figure (6), a significant ( $P < 0.05$ ) increase in CEA and CA was 15.3 percent for Gen suspension compared to other Gen formulation groups. Additionally, it is noticed that levels of CEA and CA 15.3 for surface-modified Gen phytosomes are significantly ( $P < 0.05$ ) lower than surface unmodified Gen phytosome.

From the above-mentioned results, the potential effectiveness of targeted Gen phytosomes for breast cancer treatment is related to accumulated Gen amount in the malignant organ. It is reported by Klein et al.<sup>(57)</sup> that Gen possesses a biphasic effect on cell growth particularly ER+ *in-vitro*. Where Gen can stimulate the growth of breast tumor cells at low concentrations but higher concentrations, it inhibits cell proliferation. Also, Yuan et al.<sup>(58)</sup> findings support these assumptions. Thus, it is obvious that surface-modified Gen phytosomes proved their effectiveness to deliver *in-vivo* a significant amount of Gen aglycone to the active site of the tumor compared to Gen phytosomes and Gen suspension.

In G-HA, due to the presence of free HA in the interstitium, this formulation tends to deliver a high amount of Gen to the target organs systemically as shown in figure (4). However, G-PHA tends to deliver a high amount of Gen via the lymphatic system due to the presence of MPEG<sub>2000</sub>-DSPE which improves interstitium lymphatic drainage following SC administration. These assumptions were proved by the presence high Gen amount in the target organ although the difference in pharmacokinetic behavior between G-HA and G-PHA. Hence, surface modified Gen phytosomes tend to improve the efficacy of Gen in breast cancer treatment as proved from the obtained decreased tumor size (figure 5) and tumor biomarkers (figure 6).

## Conclusion

Breast cancer-targeted Gen phytosome is a novel approach to improve cancer efficacy of Gen. SC route is reported to be a preferable route of administration for lymphatic drainage improvement and is supposed to show better chemotherapeutic action towards breast cancer.

The current study succeeded in the preparation of two surfaces modified Gen phytosomal formulations based on using HA (G-HA) alone or combined with MPEG<sub>2000</sub>-DSPE [G-PHA].

G-HA and G-PHA show a promising chemotherapeutic effect against breast cancer because of targeting properties owing to the presence of HA. Additionally, the presence of MPEG<sub>2000</sub>-DSPE results in improving interstitium lymphatic drainage and prolongation of therapeutic effects toward breast cancer. These findings are supported by lowering tumor size and the other tumor markers (CEA and CA 15.3). This opens the room for further studies to evaluate lymphatic targeting of G-PHA toward metastatic breast cancer after SC administration.

## Authorship contributions:

**Ibrahim A. Komeil:** Conceptualization, Methodology, Formal analysis, Resources, Writing - Original Draft, Writing - Review & Editing, Investigation

**Ossama Y. Abdallah:** Conceptualization, Methodology, Writing - Original Draft, Writing - Review & Editing, Supervision

**Wessam M. El-Refaie:** Conceptualization, Methodology, Writing - Original Draft, Writing - Review & Editing, Supervision, Project administration

## References

1. Waks AG, Winer EP. Breast Cancer Treatment: A Review. *JAMA - Journal of the American Medical Association*. 2019;321(3):288–300.
2. Lin NU, Amiri-Kordestani L, Palmieri D, Liewehr DJ, Steeg PS. CNS metastases in breast cancer: Old challenge, new frontiers. *Clinical Cancer Research*. 2013;19(23):6404–18.
3. Banerjee S, Li Y, Wang Z, Sarkar FH. Multi-targeted therapy of cancer by genistein. *Cancer Letters*. 2008;269(2):226–42.
4. Akiyama T, Ishida J, Nakagawa S, Ogawara H, Watanabe S, Itoh N, et al. Genistein, a specific inhibitor of tyrosine-specific protein kinases. *J Biol Chem*. 1987;262(12):5592–5.
5. Sakla MS, Shenouda NS, Ansell PJ, MacDonald RS, Lubahn DB. Genistein affects HER2 protein concentration, activation, and promoter regulation in BT-474 human breast cancer cells. *Endocrine*. 2007;32(1):69–78.

6. Yang Z, Kulkarni K, Zhu W, Hu M. Bioavailability and Pharmacokinetics of Genistein: Mechanistic Studies on its ADME. *Anti-Cancer Agents in Medicinal Chemistry*. 2012;12(10):1264–80.
7. Bhat SS, Prasad SK, Shivamallu C, Prasad KS, Syed A, Reddy P, et al. Genistein: A potent anti-breast cancer agent. Vol. 43, *Current Issues in Molecular Biology*. MDPI; 2021. p. 1502–17.
8. Tyagi N, Song YH, De R. Recent progress on biocompatible nano carrier-based genistein delivery systems in cancer therapy. Vol. 27, *Journal of Drug Targeting*. Taylor and Francis Ltd; 2019. p. 394–407.
9. Cai L, Yu R, Hao X, Ding X. Folate receptor-targeted Bioflavonoid Genistein-loaded Chitosan Nanoparticles for Enhanced Anticancer Effect in Cervical Cancers. *Nanoscale Res Lett* [Internet]. 2017 [cited 2022 Apr 19];12(1). Available from: <https://pubmed.ncbi.nlm.nih.gov/28853026/>
10. Wu B, Liang Y, Tan Y, Xie C, Shen J, Zhang M, et al. Genistein-loaded nanoparticles of star-shaped diblock copolymer mannitol-core PLGA-TPGS for the treatment of liver cancer. *Mater Sci Eng C Mater Biol Appl* [Internet]. 2016 Feb 1 [cited 2022 Apr 19];59:792–800. Available from: <https://pubmed.ncbi.nlm.nih.gov/26652434/>
11. Collnot EM, Baldes C, Schaefer UF, Edgar KJ, Wempe MF, Lehr CM. Vitamin E TPGS P-glycoprotein inhibition mechanism: influence on conformational flexibility, intracellular ATP levels, and role of time and site of access. *Mol Pharm* [Internet]. 2010 Jun 7 [cited 2022 Apr 19];7(3):642–51. Available from: <https://pubmed.ncbi.nlm.nih.gov/20205474/>
12. Zhang H, Liu G, Zeng X, Wu Y, Yang C, Mei L, et al. Fabrication of genistein-loaded biodegradable TPGS-b-PCL nanoparticles for improved therapeutic effects in cervical cancer cells. *Int J Nanomedicine* [Internet]. 2015 Mar 27 [cited 2022 Apr 19];10:2461–73. Available from: <https://pubmed.ncbi.nlm.nih.gov/25848264/>
13. J T, N X, H J, HL, Z W, L W. Eudragit nanoparticles containing genistein: formulation, development, and bioavailability assessment. *Int J Nanomedicine* [Internet]. 2011 Oct [cited 2022 Apr 19];6:2429. Available from: <https://pubmed.ncbi.nlm.nih.gov/22072878/>
14. Mendes LP, Gaeti MPN, de Ávila PHM, de Sousa Vieira M, dos Santos Rodrigues B, de Ávila Marcelino RI, et al. Multicompartimental nanoparticles for co-encapsulation and multimodal drug delivery to tumor cells and neovasculature. *Pharm Res* [Internet]. 2014 [cited 2022 Apr 19];31(5):1106–19. Available from: <https://pubmed.ncbi.nlm.nih.gov/24170281/>
15. Zhang T, Wang H, Ye Y, Zhang X, Wu B. Micellar emulsions composed of MPEG-PCL/MCT as novel nanocarriers for systemic delivery of genistein: a comparative study with micelles. *International Journal of Nanomedicine* [Internet]. 2015 Oct 1 [cited 2022 Apr 19];10:6175. Available from: </pmc/articles/PMC4598212/>
16. Pham J, Brownlow B, Elbayoumi T. Mitochondria-specific pro-apoptotic activity of genistein lipidic nanocarriers. *Mol Pharm* [Internet]. 2013 Oct 7 [cited 2022 Apr 19];10(10):3789–800. Available from: <https://pubmed.ncbi.nlm.nih.gov/23992356/>
17. Aditya NP, Shim M, Lee I, Lee Y, I'm MH, Ko S. Curcumin and genistein coloaded nanostructured lipid carriers: in vitro digestion and anti-prostate cancer activity. *J Agric Food Chem* [Internet].

2013 Feb 27 [cited 2022 Apr 19];61(8):1878–83. Available from:  
<https://pubmed.ncbi.nlm.nih.gov/23362941/>

18. Stolarczyk EU, Stolarczyk K, Łaszcz M, Kubiszewski M, Maruszak W, Olejarz W, et al. Synthesis and characterization of genistein conjugated with gold nanoparticles and the study of their cytotoxic properties. *Eur J Pharm Sci* [Internet]. 2017 Jan 1 [cited 2022 Apr 19];96:176–85. Available from: <https://pubmed.ncbi.nlm.nih.gov/27644892/>
19. Zhang XY, Lu WY. . *Cancer Biol Med*. 2014;11:247–54.
20. Oussoren C, Storm G. Liposomes to target the lymphatics by subcutaneous administration. *Advanced Drug Delivery Reviews*. 2001;50:143–56.
21. Cai S, Zhang Q, Bagby T, Forrest ML. Lymphatic drug delivery using engineered liposomes and solid lipid nanoparticles. *Adv Drug Deliv Rev*. 2011;10(63):10–1.
22. Zhuang Y, Ma Y, Wang C, Hai L, Yan C, Zhang Y, et al. PEGylated cationic liposomes robustly augment vaccine-induced immune responses: Role of lymphatic trafficking and biodistribution. *Journal of Controlled Release*. 2012;
23. Tiantian Y, Wenji Z, Mingshuang S, Rui Y, Shuangshuang S, Yuling M, et al. Study on intralymphatic-targeted hyaluronic acid-modified nanoliposome: Influence of formulation factors on the lymphatic targeting. *International Journal of Pharmaceutics*. 2014;471(1–2):245–57.
24. Biju S, Talegaonkar S, Mishra P, Khar R. Vesicular systems: An overview. *Indian Journal of Pharmaceutical Sciences*. 2006;68(2):141–53.
25. Vinod KR, Sandhya S, Chandrashekar J, Swetha R, Rajeshwar T, Banji D, et al. A review on genesis and characterization of phytosomes. *International Journal of Pharmaceutical Sciences Review and Research*. 2010;
26. Necas J, Bartosikova L, Brauner P, Kolar J. Hyaluronic acid (hyaluronan): A review. *Veterinarni Medicine*. 2008;53(8):397–411.
27. Elzoghby AO, Mostafa SK, Helmy MW, ElDemellawy MA, Sheweita SA. Superiority of aromatase inhibitor and cyclooxygenase-2 inhibitor combined delivery: Hyaluronate-targeted versus PEGylated protamine nanocapsules for breast cancer therapy. *International Journal of Pharmaceutics*. 2017;529(1–2):178–92.
28. Wong MY, Chiu GNC. Liposome formulation of co-encapsulated vincristine and quercetin enhanced antitumor activity in a trastuzumab-insensitive breast tumor xenograft model. *Nanomedicine: Nanotechnology, Biology, and Medicine*. 2011;7(6):834–40.
29. Yang Z, Zhu W, Gao S, Xu H, Wu B, Kulkarni K, et al. Simultaneous determination of genistein and its four phases II metabolites in blood by a sensitive and robust UPLC-MS/MS method: application to an oral bioavailability study of genistein in mice. *J Pharm Biomed Anal*. 2010;53(1):81–9.
30. Komeil IA, El-Refaie WM, Gowayed MA, El-Ganainy SO, El Achy SN, Huttunen KM, et al. Oral genistein-loaded phytosomes with enhanced hepatic uptake, residence and improved therapeutic efficacy against hepatocellular carcinoma. *International Journal of Pharmaceutics*. 2021 May 15;601:120564.

31. Allam AN, Komeil IA, Abdallah OY. Curcumin phytosomal softgel formulation: Development, optimization and physicochemical characterization. *Acta Pharmaceutica*. 2015;65(3):285–97.
32. Allam AN, Komeil IA, Fouda MA, Abdallah OY. Preparation, characterization, and in vivo evaluation of curcumin self-nano phospholipid dispersion as an approach to enhance oral bioavailability. *International Journal of Pharmaceutics*. 2015;489(1–2):117–23.
33. Zhuang Y, Ma Y, Wang C, Hai L, Yan C, Zhang Y, et al. PEGylated cationic liposomes robustly augment vaccine-induced immune responses: Role of lymphatic trafficking and biodistribution. *Journal of Controlled Release*. 2012;159(1):135–42.
34. Hosoda K, Furuta T, Ishii K. Simultaneous determination of glucuronic acid and sulfuric acid conjugated metabolites of daidzein and genistein in human plasma by high-performance liquid chromatography. *Journal of Chromatography B: Analytical Technologies in the Biomedical and Life Sciences*. 2010;878(7–8):628–36.
35. El-Mezayen NS, El-Hadidy WF, El-Refaie WM, Shalaby ThI, Khatib MM, El-Khatib AS. Hepatic stellate cell-targeted imatinib nanomedicine versus conventional imatinib: A novel strategy with potent efficacy in experimental liver fibrosis. *Journal of Controlled Release*. 2017;266:226–37.
36. Shehata EMM, Elnaggar YSR, Galal S, Abdallah OY. Self-emulsifying phospholipid pre-concentrates (SEPPs) for improved oral delivery of the anti-cancer genistein: Development, appraisal and ex-vivo intestinal permeation. *International Journal of Pharmaceutics* [Internet]. 2016;511(2):745–56. Available from: <http://dx.doi.org/10.1016/j.ijpharm.2016.07.078>
37. Elnaggar YSR, Shehata EMM, Galal S, Abdallah OY. Self-emulsifying pre-concentrates of the daidzein-phospholipid complex: Design, in vitro and in vivo appraisal. *Nanomedicine*. 2017;12(8):893–910.
38. Freag MS, Elnaggar YSR, Abdelmonsif DA, Abdallah OY. Layer-by-layer-coated lyotropic liquid crystalline nanoparticles for active tumor targeting of rapamycin. *Nanomedicine*. 2016;11(22):2975–96.
39. Kabel AM. Tumor markers of breast cancer: New prospectives. *Journal of Oncological Sciences*. 2017;3(1):5–11.
40. Ali Khan A, Mudassir J, Mohtar N, Darwis Y. Advanced drug delivery to the lymphatic system: lipid-based nanoformulations. *Int J Nanomedicine*. 2013;8:2733–44.
41. Cannavà C, Crupi V, Ficarra P, Guardo M, Majolino D, Mazzaglia A, et al. Physico-chemical characterization of an amphiphilic cyclodextrin/genistein complex. *Journal of Pharmaceutical and Biomedical Analysis*. 2010;51(5):1064–8.
42. Silverstein R, Webster F, Kiemle D. *Spectrometric Identification of Organic Compounds*. Seventh Ed. New York: John Wiley & Son;
43. Danciu C, Soica C, Dehelean C, Zupko I, Csanyi E, Pinzaru I. Preliminary In Vitro Evaluation of Genistein Chemopreventive Capacity as a Result of Esterification and Cyclodextrin Encapsulation. *Analytical Cellular Pathology*. 2015;2015:1–8.

44. Knudsen KB, Northeved H, Pramod Kumar EK, Permin A, Getting T, Andresen TL, et al. In vivo toxicity of cationic micelles and liposomes. *Nanomedicine: Nanotechnology, Biology, and Medicine*. 2015;11(2):467–77.
45. El-Refaie WM, Elnaggar YSR, El-Massik MA, Abdallah OY. Novel Self-assembled, Gel-core Hyaluosomes for Non-invasive Management of Osteoarthritis: In-vitro Optimization, Ex-vivo and In-vivo Permeation. *Pharmaceutical Research*. 2015;32(9):2901–11.
46. Yang T, Cui F De, Choi MK, Cho JW, Chung SJ, Shim CK, et al. Enhanced solubility and stability of PEGylated liposomal paclitaxel: In vitro and in vivo evaluation. *International Journal of Pharmaceutics*. 2007;338(1–2):317–26.
47. Phan V, Walters J, Brownlow B, Elbayoumi T. Enhanced cytotoxicity of optimized liposomal genistein via specific induction of apoptosis in breast, ovarian and prostate carcinomas. *Journal of Drug Targeting*. 2013;21(10):1001–11.
48. Crosasso P, Ceruti M, Brusa P, Arpicco S, Dosio F, Cattel L. Preparation, characterization and properties of sterically stabilized paclitaxel-containing liposomes. *Journal of Controlled Release*. 2000;63(1–2):19–30.
49. Yang T, Choi MK, Cui F De, Kim JS, Chung SJ, Shim CK, et al. Preparation and evaluation of paclitaxel-loaded PEGylated immunoliposome. *Journal of Controlled Release*. 2007;120(3):169–77.
50. Franzen U, Vermehren C, Jensen H, Østergaard J. Physicochemical characterization of a PEGylated liposomal drug formulation using capillary electrophoresis. *Electrophoresis*. 2011;32(6–7):738–48.
51. Li R, Liu H, Huang H, Bi W, Yan R, Tan X, et al. Chitosan conduit combined with hyaluronic acid prevent sciatic nerve scar in a rat model of peripheral nerve crush injury. *Molecular Medicine Reports*. 2018;17(3):4360–8.
52. Patel HM, Katherine M. B, Vaughan-Jones R. Assessment of the potential uses of liposomes for lymphoscintigraphy and lymphatic drug delivery failure of 99m-technetium marker to represent intact liposomes in lymph nodes. *Biochimica et Biophysica Acta (BBA) - General Subjects* [Internet]. 1984 [cited 2019 Aug 19];801(1):76–86. Available from: <http://www.ncbi.nlm.nih.gov/pubmed/6087919>
53. Hawley AE, Davis SS, Illum L. Targeting of colloids to lymph nodes: influence of lymphatic physiology and colloidal characteristics. *Advanced Drug Delivery Reviews*. 1995;17(1):129–48.
54. Patel HM. Serum opsonins and liposomes: their interaction and opsonophagocytosis. *Crit Rev Ther Drug Carrier Syst*. 1992;9(1):39–90.
55. Elzoghby AO, Mostafa SK, Helmy MW, ElDemellawy MA, Sheweita SA. Multi-Reservoir Phospholipid Shell Encapsulating Protamine Nanocapsules for Co-Delivery of Letrozole and Celecoxib in Breast Cancer Therapy. *Pharmaceutical Research*. 2017;34(9):1956–69.
56. Elzoghby AO, El-Lakany SA, Helmy MW, Abu-Serie MM, Elgindy NA. Shell-crosslinked zein nanocapsules for oral codelivery of exemestane and resveratrol in breast cancer therapy. *Nanomedicine*. 2017;12(24):2785–805.

57. Klein C, King A. Genistein genotoxicity: Critical considerations of in vitro exposure dose. *Toxicology and Applied Pharmacology*. 2007;224(1):1–11.
58. Yuan B, Wang L, Jin Y, Zhen H, Xu P, Xu Y, et al. Role of metabolism in the effects of genistein and its phase II conjugates on the growth of human breast cell lines. *AAPS Journal*. 2012;14(2):329–44.

### **Figures legends:**

Figure 1: [A] Infra-red spectra and [B] DSC thermograms, each shows the spectra of Gen, Lipoid S-100, Gen-SPC complex, and the physical mixture.

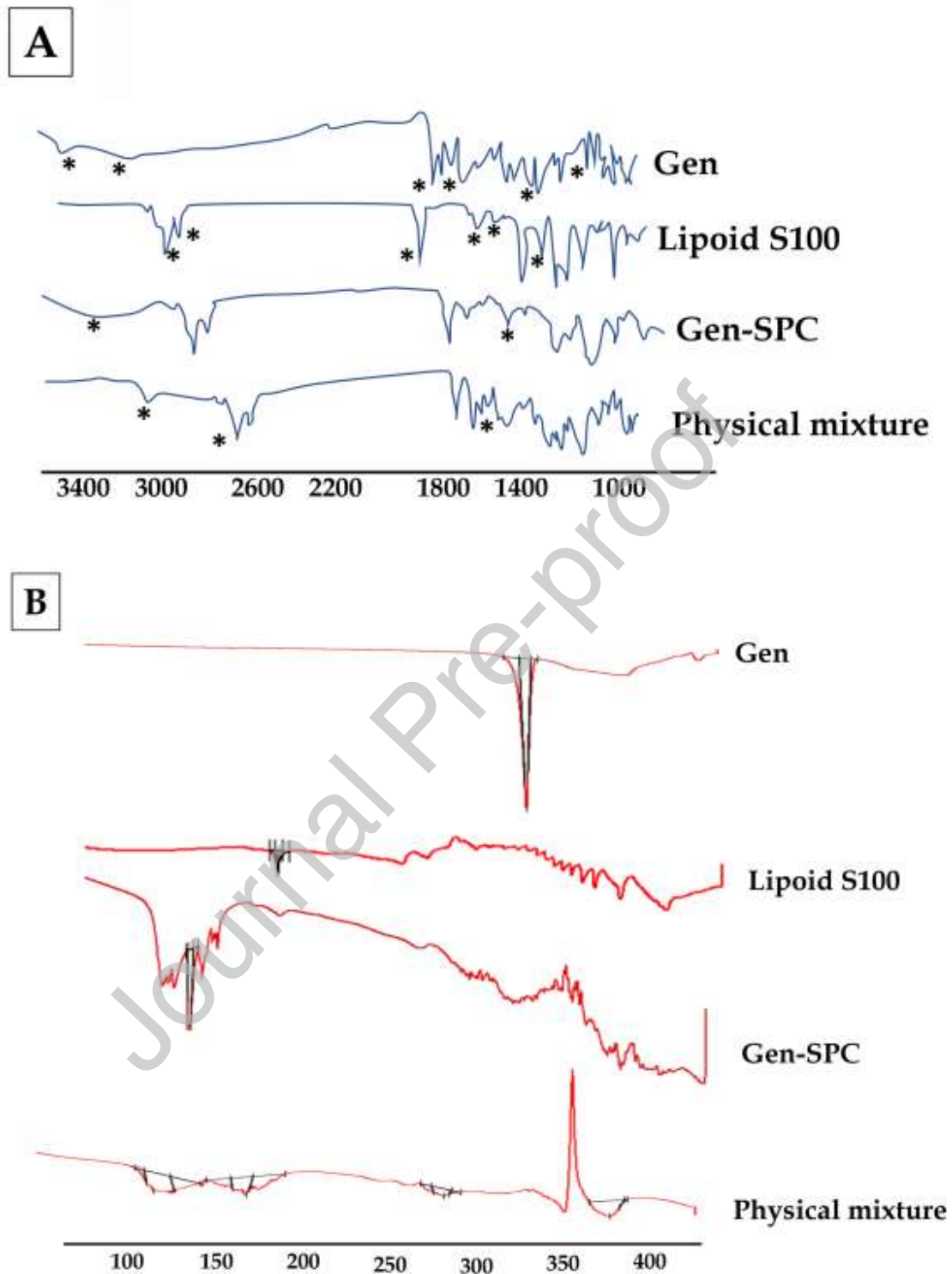
Figure 2: Transmission electron microscopic photograph of [A] Gen phytosomes, [B] G-HA, [C], and [D] G-PHA with 500 folds dilution in distilled water.

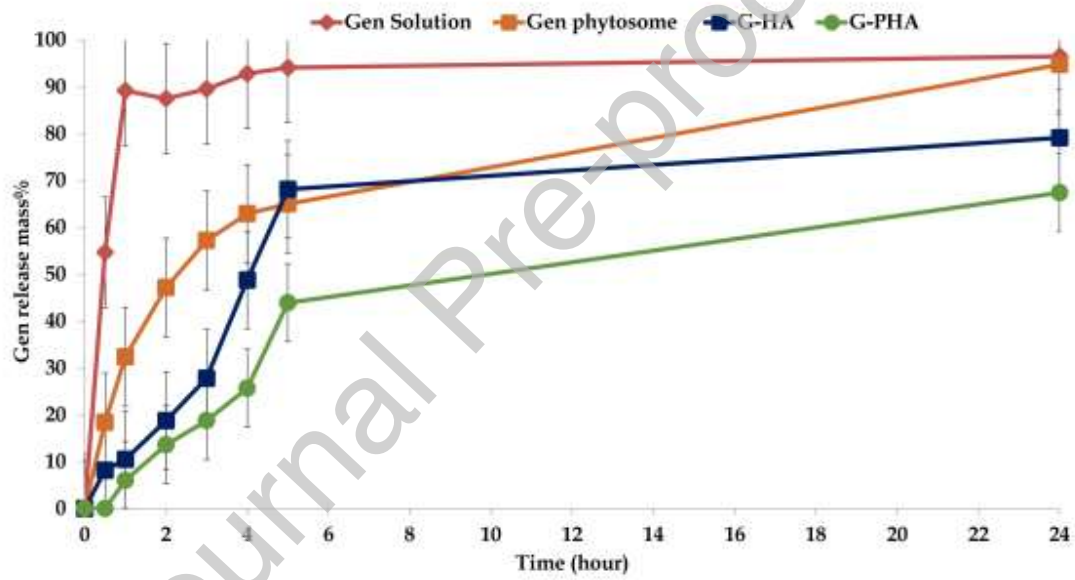
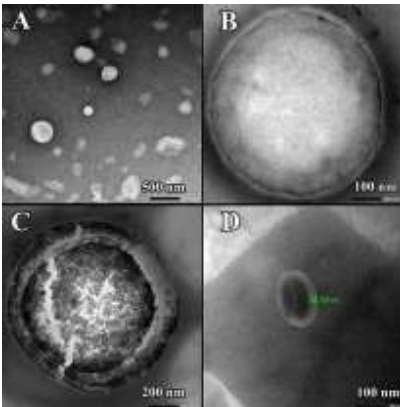
Figure 3: *In-vitro* drug release from Gen-phytosomal formulations using dialysis bag method and phosphate buffer pH 6.8 with 0.1% Tween [w/v] as a receiver medium, Data expressed as mean  $\pm$  SD [n=3].

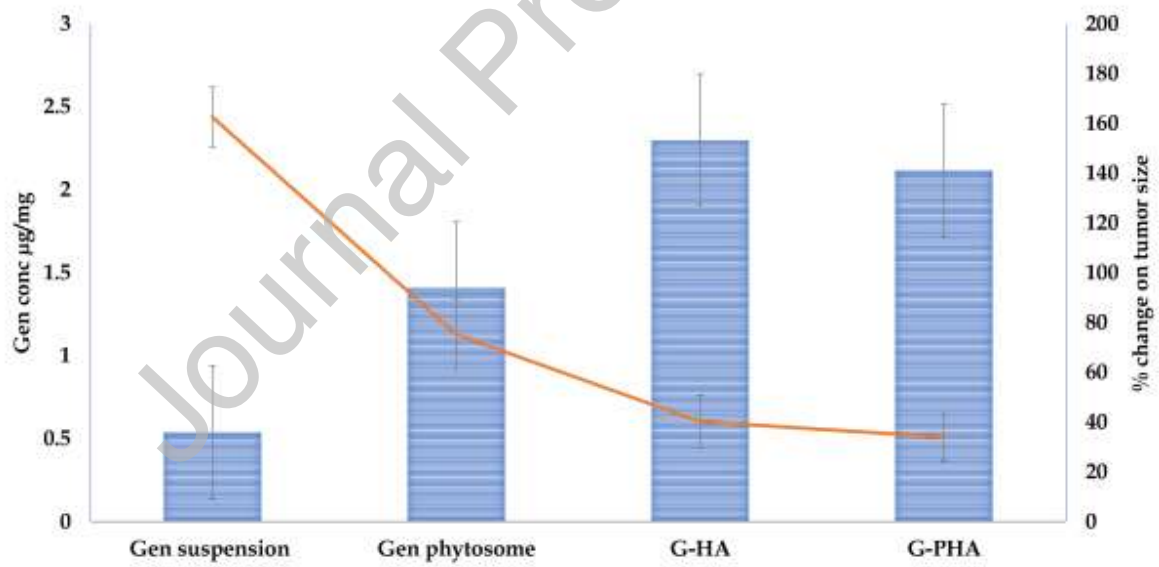
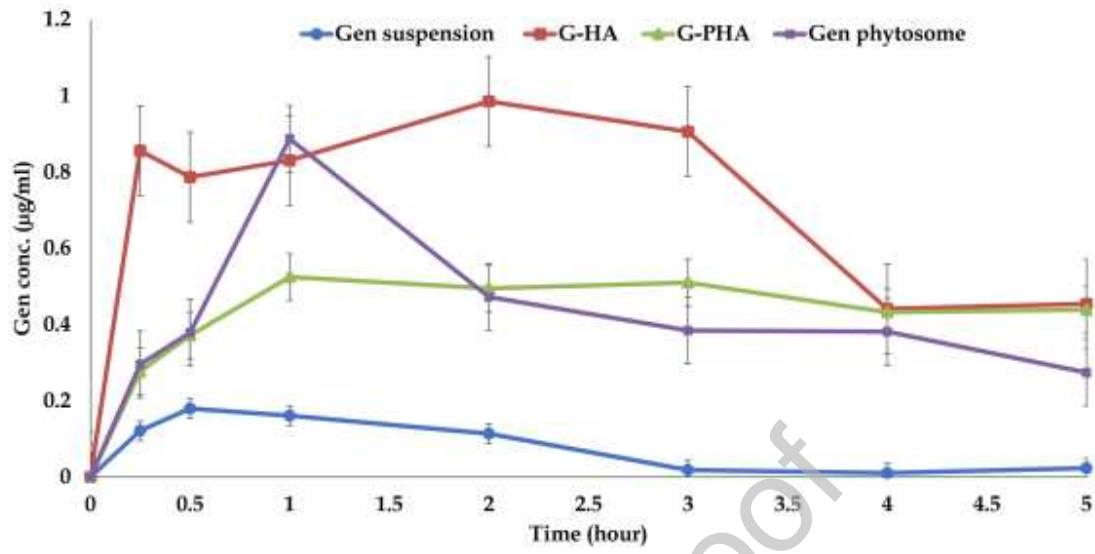
Figure 4: Graphical presentation for Gen aglycone in plasma after SC injection with Gen phytosomes, G-HA and G-PHA.

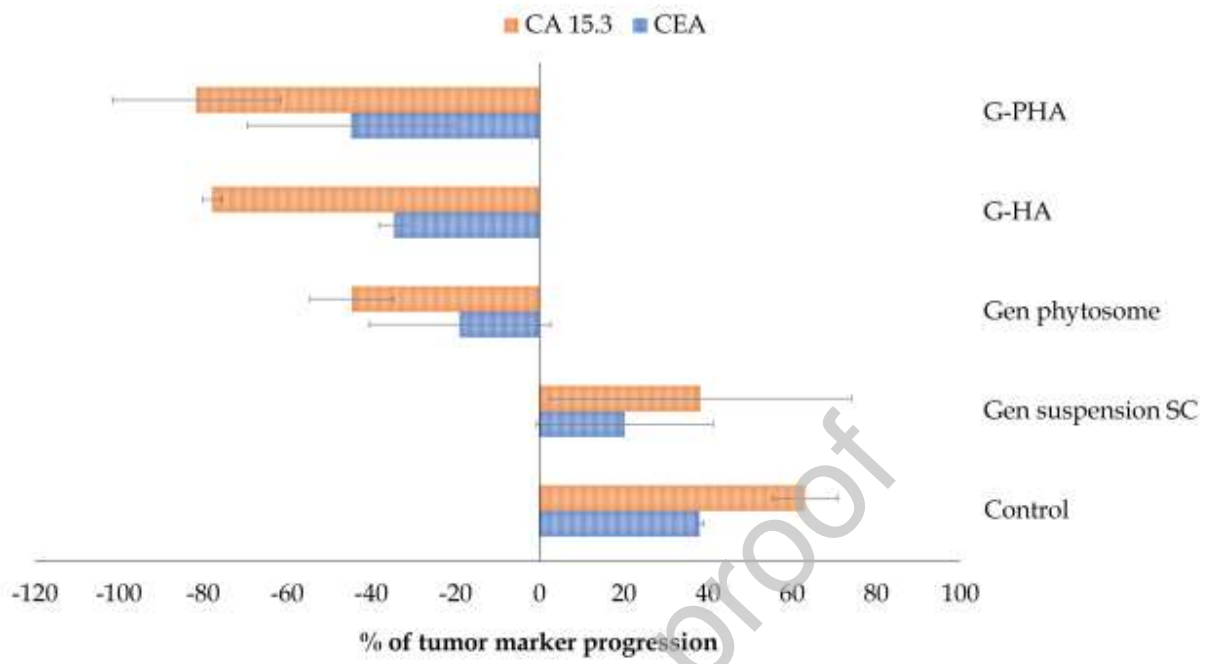
Figure 5: Graphical presentation for Gen aglycone disposition in the isolated mammary gland and percentage change of tumor size at the end of treatment with Gen suspension, Gen phytosomes, G-HA, and G-PHA.

Figure 6: Percentage of change of tumor markers [CEA and CA 15.3] at the end of treatment with Gen suspension, Gen phytosomes, G-HA, and G-PHA.









**Table 1:** Results of content, PS, PDI, and ZP of targeted Gen phytosomal formulations, values are presented as (mean  $\pm$  SD, n=3)

Formula No.	Gen content (mg %)	PS (nm)	PDI	ZP
Gen-phytosomes	85%	230.5 $\pm$ 10.6	0.158 $\pm$ 0.054	-25.32 $\pm$ 0.568
G-HA	92%	144.2 $\pm$ 1.266	0.182 $\pm$ 0.021	-30.92 $\pm$ 0.754
G-PHA	90%	220.3 $\pm$ 2.516	0.291 $\pm$ 0.011	-32.06 $\pm$ 0.305

**Table 2:** Primary and secondary pharmacokinetic parameters for free Gen aglycone detected in blood after SC injection of Gen suspension, Gen-phytosome, G-HA, and G-PHA, values represented as Mean  $\pm$  SD (n=5)

Formula No.	PK P. [unit]	Free Gen aglycone	
		Mean	$\pm$ SD
<b>Gen suspension</b>	C <sub>max</sub> $\mu$ g/ml	0.202	0.016
	AUC <sub>0-t</sub> $\mu$ g/ml*h	0.374	0.085
	T <sub>max</sub> hr	1	N/A
	T <sub>1/2</sub> hr	1.141	0.225
<b>Gen phytosome</b>	C <sub>max</sub> $\mu$ g/ml	0.888	0.207
	AUC <sub>0-t</sub> $\mu$ g/ml*h	2.257	0.213
	T <sub>max</sub> hr	1	N/A
	T <sub>1/2</sub> hr	3.287	0.909
<b>G-HA</b>	C <sub>max</sub> $\mu$ g/ml	0.959	0.054
	AUC <sub>0-t</sub> $\mu$ g/ml*h	3.563	0.067
	T <sub>max</sub> hr	0.25	N/A
	T <sub>1/2</sub> hr	2.136	0.345
<b>G-PHA</b>	C <sub>max</sub> $\mu$ g/ml	0.505	0.012
	AUC <sub>0-t</sub> $\mu$ g/ml*h	2.092	0.058
	T <sub>max</sub> hr	3	N/A
	T <sub>1/2</sub> hr	7.379	0.938